ORNL/TM-2023/2886

A Review of Advanced Test Reactor Fuel and Assessment of Its Compatibility with the ZIRCEX Chlorination Process

OAK RIDGE NATIONAL LABORATORY
MANAGED BY UT BATTELLE
FOR U.S. DEPARTMENT OF ENERGY

Jacob A. Hirschhorn
Joanna McFarlane

April 2023

OAK RIDGE
National Laboratory

ORNL IS MANAGED BY UT-BATTELLE LLC FOR THE US DEPARTMENT OF ENERGY

DOCUMENT AVAILABILITY

Reports produced after January 1, 1996, are generally available free via OSTI.GOV.

Website www.osti.gov

Reports produced before January 1, 1996, may be purchased by members of the public from the following source:

National Technical Information Service
5285 Port Royal Road
Springfield, VA 22161
Telephone 703-605-6000 (1-800-553-6847)
TDD 703-487-4639
Fax 703-605-6900
E-mail info@ntis.gov
Website http://classic.ntis.gov/

Reports are available to US Department of Energy (DOE) employees, DOE contractors, Energy Technology Data Exchange representatives, and International Nuclear Information System representatives from the following source:

Office of Scientific and Technical Information
PO Box 62
Oak Ridge, TN 37831
Telephone 865-576-8401
Fax 865-576-5728
E-mail reports@osti.gov
Website https://www.osti.gov/

This report was prepared as an account of work sponsored by an agency of the United States Government. Neither the United States Government nor any agency thereof, nor any of their employees, makes any warranty, express or implied, or assumes any legal liability or responsibility for the accuracy, completeness, or usefulness of any information, apparatus, product, or process disclosed, or represents that its use would not infringe privately owned rights. Reference herein to any specific commercial product, process, or service by trade name, trademark, manufacturer, or otherwise, does not necessarily constitute or imply its endorsement, recommendation, or favoring by the United States Government or any agency thereof. The views and opinions of authors expressed herein do not necessarily state or reflect those of the United States Government or any agency thereof.

ORNL/TM-2023/2886

Nuclear Energy and Fuel Cycle Division

A REVIEW OF ADVANCED TEST REACTOR FUEL AND ASSESSMENT OF ITS COMPATIBILITY WITH THE ZIRCEX CHLORINATION PROCESS

Jacob A. Hirschhorn
Joanna McFarlane

April 2023

Prepared by
OAK RIDGE NATIONAL LABORATORY
Oak Ridge, TN 37831
managed by
UT-BATTELLE LLC
for the
US DEPARTMENT OF ENERGY
under contract DE-AC05-00OR22725

CONTENTS

ABBREVIATIONS iv
ACKNOWLEDGMENTS v
ABSTRACT 1
1. INTRODUCTION 1
2. ADVANCED TEST REACTOR BACKGROUND 2
3. ADVANCED TEST REACTOR FUEL 3
    3.1 DIMENSIONS 4
    3.2 FABRICATION 4
    3.3 FRESH FUEL COMPOSITION 5
    3.4 BURNUP 6
    3.5 IRRADIATION EFFECTS 7
    3.6 FISSION PRODUCT CONTENT 8
4. OPEN QUESTIONS 9
5. CONCLUSIONS 10
REFERENCES 11

ABBREVIATIONS

ATR	Advanced Test Reactor
CIC	core internals changeout
DOE	US Department of Energy
HALEU	high-assay low-enriched uranium
ICSBEP	International Criticality Safety Benchmark Evaluation Project
INL	Idaho National Laboratory
LEU	low-enriched uranium
NEA	Nuclear Energy Agency
ORNL	Oak Ridge National Laboratory
SNF	spent nuclear fuel
TRISO	tristructural-isotropic
ZIRCEX	zirconium removal prior to extraction

ACKNOWLEDGMENTS

This work was funded by the US Department of Energy Office of Nuclear Energy, Materials Recovery and Waste Forms Program, NE-43.

ABSTRACT

Advanced Test Reactor (ATR) fuel has been identified as a resource for high-assay low-enriched uranium (HALEU) production. A survey was performed on the published literature describing ATR fuel. The geometry of the fuel is complex; different parts of the fuel compact experience differing neutron flux and burnup. The literature is sparse, and access is controlled. Therefore, fundamental studies of fuel reprocessing must use a model fuel that represents the main chemical and structural features. Advanced chlorination, or chlorination with sulfur-chlorine bearing reagents is being investigated as way to separate the fuel from metal matrix alloys.

A UAl_x alloy will be fabricated with $x = 3$, 4, and 5. The potential chlorination of individual UAl_x intermetallics will be assessed in the advanced chlorination process of Al-8001 and Al-6061 as well as a representative mixture. Initial studies will track the alloying elements of the Al, which are Si, Fe, Cu, Mn, Mg, Cr, Zn, and Ti, in addition to the U itself. Further studies will include fission product simulants. Because advanced chlorination solvents include sulfur, the chemistry of sulfur with major and minor constituents will also be investigated. The experimental work accompanied by neutronic calculations will allow the assessment of the feasibility of advanced chlorination to separate aluminum from uranium. If bench-scale testing appears promising, then small-scale tests in shielded facilities with irradiated cladding, lightly irradiated fuel, and spent nuclear fuel are recommended to track the complete inventory of fissile actinides, fission product impurities, and reagent solids and liquids.

1. INTRODUCTION

Demand for high-assay low-enriched uranium (HALEU) with enrichments of 5%–20% is expected to grow significantly by 2030 and beyond [1]. HALEU applications include microreactors, advanced reactor fuels such as tristructural-isotropic (TRISO) particles, extending the operating cycles of existing oxide-fueled reactors and other US Department of Energy (DOE) missions [1, 2]. DOE is pursuing several options to help develop a domestic supply chain for HALEU. Short-term solutions involve recovering U from spent nuclear fuels (SNFs) containing highly enriched U. Uranium can be recovered from (1) metallic alloy fuels from Experimental Breeder Reactor II using an electrometallurgical treatment process, and (2) some metallic alloy and composite fuels from research and test reactors using the zirconium removal prior to extraction (ZIRCEX) process [1]. Establishment of domestic enrichment capabilities is expected to satisfy long-term demands for HALEU.

Uranium recovery via the ZIRCEX process is expected to proceed according to the following steps: (1) removal of Zr and/or Al cladding and/or fuel alloy constituents, (2) separation of U from fission products via a solvent extraction system, (3) downblending of U to enrichments appropriate for HALEU, (4) U solidification, and (5) fuel fabrication [3]. The current work is concerned with only the first step of this process. Preliminary testing has been conducted using unirradiated and irradiated samples to demonstrate the feasibility of this process and to assess the associated chemical reaction rates [3]. The goal of the current work is to further refine the process by demonstrating adequate control of fission products when processing realistic SNFs. This work is part of an ongoing collaboration across multiple national laboratories and university partners [3, 4]. This report focuses on work being performed at Oak Ridge National Laboratory (ORNL) and the University of Tennessee. Details on the chlorination reactions applied to zirconium and zirconium alloys has been published by Vestal and colleagues [5].

SNF from the Advanced Test Reactor (ATR) was selected for this stage of the project because of its potential compatibility with the ZIRCEX process and ongoing efforts to manage SNF from ATR [6, 7]. A literature review was conducted to collect supporting information related to ATR and its fuel's geometry, composition, and expected fission product content. The findings of the review are detailed below.

2. ADVANCED TEST REACTOR BACKGROUND

ATR is a high-flux test reactor at Idaho National Laboratory (INL) which began full power operation in 1969 [8] and is currently operated as a National Science User Facility [9]. Its missions include supporting lifetime extensions for existing reactors and advanced reactor development through studying the effects of irradiation on fuels and structural materials [8, 9]. ATR also produces radioactive isotopes for medical and industrial applications [8].

The maximum power output of ATR is 250 MW_{th}, but it is more frequently operated at approximately 110 MW_{th} to meet the needs of its current customers [10]. It is a light-water moderated, Be reflected, pressurized water reactor with maximum thermal and fast neutron fluxes of about 1.0×10^{15} and 5.0×10^{14} n/cm^2-s, respectively [8, 9]. ATR nominally operates 75% of the year, and its average cycle length is approximately 49 days [10].

ATR uses 40 fuel elements arranged in a four-lobed serpentine annulus configuration [8]. Each fuel element contains 19 fuel plates. An overhead view of the ATR core, detailed views of an ATR fuel element and fuel plate, and a cross-sectional micrograph of a fuel plate similar to that used in ATR are shown in the upper left, bottom, and upper right corners of Figure 1, respectively [8, 11]. The micrograph illustrates the macroscopic fuel and cladding regions of the fuel plate and reveals the microstructure of the composite fuel region, which is discussed further in the next section. The reactor has a constant axial power profile [10], and the serpentine lobes can be operated independently at different powers as needed to facilitate irradiation experiments and isotope production [9]. ATR fuel is described in detail throughout Section 3.

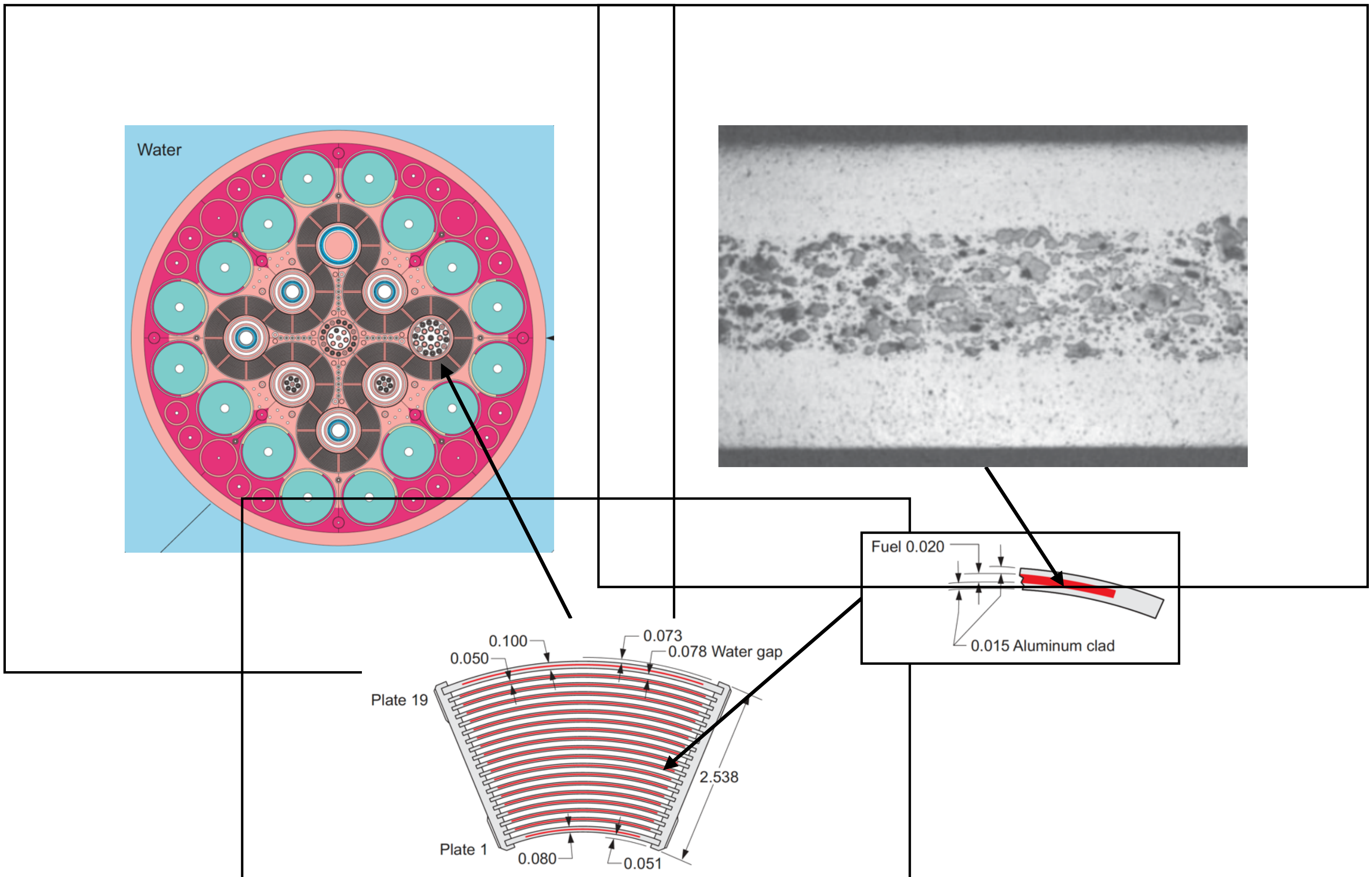

Figure 1. Overhead views of the ATR core (upper left) [8], detailed views of an ATR fuel element and fuel plate (bottom, dimensions in inches) [8], and a cross-sectional micrograph of a fuel plate similar to that used in ATR (upper right, scale not specified) [11].

3. ADVANCED TEST REACTOR FUEL

General information on past and current ATR fuel forms has been reported by Nigg and Steuhm [12]. A general discussion is provided below, followed by more detail in subsequent subsections.

ATR fuel plates contain composite fuels consisting of U-bearing particles suspended in Al matrices [12]. The composite fuels are then clad in Al. The Mark I through Mark V ATR fuel designs contained U_3O_8 particles, which were replaced with uranium aluminide (UAl_x) particles in the Mark VI and Mark VII (current) designs.

As of 2017, there were 976 spent fuel elements in wet storage (including the spent fuel canal and spent fuel pool) and 2,008 spent fuel elements in dry storage. An additional 105 spent fuel elements are generated each year [7]. Because the current Mark VII fuel design was adopted relatively quickly compared to the overall age of ATR, the majority of ATR SNF contains UAl_x [12]. The authors recommend that tests conducted in this stage of the project focus on UAl_x-bearing ATR fuel because of its abundance in the SNF inventory and its presumed compatibility with the ZIRCEX process compared to U_3O_8-bearing ATR fuel.

This work focuses on the Mark VII fuel design. Information related to legacy fuel forms is considered only as needed to supplement the Mark VII fuel literature [13–15]. An ongoing effort is under way to convert the ATR core to low-enriched uranium (LEU) [16, 17]. The fuel forms associated with the proposed LEU conversion are not considered herein.

The four variations of the Mark VII fuel design all use UAl_x-Al composite fuels clad in Al [12]. XA fuel elements are the most common. These are often referred to *zone-loaded fuel elements* because they contain variable concentrations of ^{10}B, which acts as a burnable poison for reactivity control. A nonborated version of the XA fuel element, denoted *NB*, is the next most common. Only about five NB fuel elements are used per year. YA fuel elements are identical to XA elements, except that Plate 19 does not contain fuel. About 20 YA fuel elements are used per core internals changeout (CIC) cycle (approximately 10–12 years). The final fuel element type is denoted as YA-M. YA-M fuel elements feature smaller side plate widths and are used when the Be reflector has aged and swollen.

The authors recommend that tests conducted during this stage of the project focus on XA zone–loaded fuel elements because of their abundance in the ATR SNF inventory. Inclusion of other fuel variations will change the relative amounts of fission products, but the chemistry of the fission product will remain the same. The following subsections detail information related to the dimensions, fabrication techniques, composition, burnup, irradiation effects, and fission product content of XA fuel elements.

3.1 DIMENSIONS

The overall length of an ATR fuel element, including the boxes on upper and lower ends, is 167 cm [8]. Each of the 19 fuel plates has an overall length of 125.7 cm, an active fuel length of 121.9 cm, and a fuel region thickness of 0.51 mm. Plates 1, 2–18, and 19 have overall thicknesses of 2.03 mm, 1.27 mm, and 2.54 mm, respectively. More detailed dimensions with tolerances are available in the literature [8]. Note that *plate widths* given in the literature refer to the lengths of the arcs transcribed by the plates.

Because of the geometry of the ATR fuel element, the quantities and relative concentrations of U, Al, and other elements vary between plates. This observation may have an important implication for chemical processing of ATR SNF. The process needed to treat an entire fuel element may be very different from the process needed to treat a single fuel plate or segment of a fuel plate. These implications should be explored further as the process is refined and scaled up.

3.2 FABRICATION

Most of the open literature related to fabrication of ATR fuel and similar uranium aluminide dispersion fuels focuses on preparation and handling of uranium aluminide particles. The uranium aluminide phases and their crystal structures, densities, and melting temperatures are shown in Table 1 [11, 18]. Additional thermomechanical properties are available in the literature [18]. Inconsistencies in the phases are reported in the U-Al binary phase diagrams. In 1950, Gordon and Kaufmann reported that UAl_5 was stable and that UAl_4 was not [19]. A later study published in 1958 reported that the stable uranium aluminides include UAl_2, UAl_3, and UAl_4 [20]. The discrepancy may be related to crystalline defects in the UAl_4 lattice, which displace U atoms and produce a U:Al stoichiometry closer to 1:5 [14].

Table 1. Uranium aluminides and their crystal structures, densities, and melting temperatures [11, 18]

Phase	Crystal structure	Density ($g{\cdot}cm^{-3}$)	Melting temperature (°C)
UAl_2	Face-centered cubic	8.1	1,590
UAl_3	Simple cubic	6.7	1,350
UAl_4	Orthorhombic	6.0	730

Uranium aluminides are prepared by vacuum induction melting, arc melting, casting, or reaction of uranium hydride with Al [11, 18]. UAl_2 content has been shown to decrease relative to that of the other uranium aluminides [21]. UAl_2 has been observed to react quickly with excess Al during fabrication and processing to form UAl_3 or UAl_4 [21] [18]. UAl_3 has been observed to react more slowly to form UAl_4 [18] as shown in Reaction (1), which is a temperature-dependent process. Similar reactions presumably occur within the reactor, particularly as fission of U atoms decreases the U:Al ratio.

$$UAl_3 + Al \rightarrow UAl_4 \tag{1}$$

A description is available of the fabrication at ORNL of ATR plates instrumented with thermocouple wells for in-core heat transfer tests [22]. Erwin and colleagues provide details of preparing instrumented plates to replace plates 15/16 and 17/18 in a fuel assembly [22]. The manufacturing procedure was modified from the standard conditions, which included preparation of stoichiometric UAl_3 rather than a mixture of aluminides, roll bonding of dual-cored plates to accommodate thermocouples, and marforming in compression. The ATR plates are described in the open literature and are summarized here.

The uranium aluminides were fabricated using a powder metallurgy technique [22] which includes (1) mixing uranium hydride in an excess of aluminum, (2) pressing the blend in a graphite die heated to 1,000°C in argon to remove the hydrogen, and (3) crushing and screening the mixture to a desired particle size.

After analysis was conducted to confirm the composition, the mixture was then mixed with other constituent powders and pressed at 3,100 bar into fuel compacts. These compacts were vacuum degassed with temperatures up to 525°C. Some swelling of the UAl_x material occurred during this step (approximately 4%).

The curved fuel plates were then formed by roll swaging [8]. Three compacts were used per plate, which were added to the billet, sequentially. The compacts were sealed and annealed between loadings. When assembled, the billets were heated to 500°C and rolled in a hot reduction process [22]. The billets were rolled in different directions until they reached a thickness of 5.6 mm. Holes were drilled for thermocouples, and the curved plates were formed by lateral compression into the required shape.

3.3 FRESH FUEL COMPOSITION

Fresh ATR fuel is enriched to 93 wt% [8]. Note that ATR fuel is irradiated to burnups of about 10–50 at% [23], leaving a varied isotopic composition. ATR SNF inputs into the ZIRCEX process would therefore have significantly lower enrichments, and the enrichments of different fuel assemblies and plates may vary significantly. Fuel burnup is discussed further below.

Composition standards are established for fresh ATR fuel and its precursors [12]. Limits are placed on the Cd, Li, B, Si+Fe, Zn, Cu, and Al_2O_3 contents of the Al powders used to produce UAl_x [8]. Similarly, limits are placed on O, C, N, H, and fatty and oily matter contents of the UAl_x powder [8]. The content limits sum to 1.045 wt%. Limits are also placed on the contents of other impurities in terms of their ^{10}B equivalents to minimize the effects of impurities on reactivity. However, B_4C is deliberately added to the UAl_x powder in a ratio of 0.5 wt% ^{235}U: B_4C [22]. The fuel matrix is fabricated from Al-8001 [7].

UAl_x powder lots typically contain about 8 wt% UAl_2, 78 wt% UAl_3, and 14 wt% UAl_4 [12]. The final UAl_x powder is required to have >50 wt% UAl_3. The final UAl_x powder should contain about 70 wt% U and 30 wt% Al. At this time, it is not understood if the U–Al atom coordination will affect reactions between the fuel and Cl during the ZIRCEX process.

Plates 1–4 and 16–19 are doped with ^{10}B, which is introduced in the form of B_4C [8, 12]. The nominal U and B loadings of each plate are provided in the literature [12]. Limits are placed on the B, C, B_2O_3, Fe, Al, Ca, Mg, and moisture contents of B_4C [8].

The cladding and other fuel assembly components are fabricated from Al-6061 [12]. The upper and lower fuel assembly adapters are T6 temper, and all other components are O temper (ASTM specification B209 [8]). In addition to Al, Al-6061 contains Si, Fe, Cu, Mn, Mg, Cr, Zn, and Ti [8]. The contents of minor alloying elements and impurities sum to 2.91 wt%. Limits are also placed on the Cd, Li, Co, and B contents of the cladding. The minor elements in Al-8001 and Al-6061 are given in Table 2.

The fuel regions of Plates 1–4 and 16–19 are fabricated with 3–11 and 4–11 vol% voids, respectively [8]. Fabrication porosity has an important effect on the irradiation behavior of the fuel. This is discussed further below.

Table 2. Composition of selected aluminum alloys [24]

Elements	Al 6061 (%)	Al 8001 (%)	MX8001
Aluminum	95.8–98.6	98.3	98.4
Chromium	0.040–0.35 (0.25)		
Copper	0.15–0.40 (0.25)	<= 0.15 (260 ppm)	
Iron	<= 0.70	0.45–0.70 (0.48)	(0.53)
Magnesium	0.80–1.2 (1.0)		
Nickel		0.90–1.3 (1.19)	(0.93)
Silicon	0.40–0.80 (0.6)	<= 0.17 (0.06)	(0.003)
Titanium	<= 0.15		(0.11)

3.4 BURNUP

Average neutron flux in an ATR has been measured using U-Al fission wires, giving a fast neutron flux of between 5×10^{-8} and 5×10^{-9} n cm^{-2} s^{-1} [25]. However, these numbers are lower than reported elsewhere: thermal and fast neutron fluxes are reported to be above 10^{12} n cm^{-2} s^{-1} [26]. The results were confirmed by beta particle counting and gamma spectroscopy of the generated fission products. ATR SNF belongs to a group of SNF with an average burnup of about 250 GWd·MTU^{-1} [6]. ATR fuel burnup can be calculated using a ^{148}Nd method, an isotopic gamma scan method, and power/depletion modeling [23]. Burnups of 10–50 at% and up to about 1.5×10^{21} f·cm^{-3} have been reported. Burnups vary throughout and between fuel plates.

Simple examples of average fuel burnup calculation and conversion to various units are provided below. The examples are based on an ATR operating continuously at a uniform power level of 250 MW for 60 days. The examples use enrichments of 93.0 wt%, a ^{235}U mass density of 1.6 g·cm^{-3}, a ^{235}U mass of 1,075 g per fuel element, and 40 fuel elements per core [8]. The remainder of the U is assumed to be ^{238}U, and the energy release from thermal neutron–induced fission is assumed to be 200 MeV. The average fission density accumulated over time is calculated as follows:

$$(250\ \cancel{MW})(60\ \cancel{d})\left(\frac{10^6\ \cancel{W}}{\cancel{MW}}\right)\left(\frac{24\ \cancel{hr}}{\cancel{d}}\right)\left(\frac{3600\ \cancel{s}}{\cancel{hr}}\right)\left(\frac{\cancel{J}}{\cancel{W\text{-}s}}\right)\left(\frac{6.242\cdot 10^{18}\ \cancel{eV}}{\cancel{J}}\right)\left(\frac{\cancel{MeV}}{10^6\ \cancel{eV}}\right) \tag{1}$$

$$\times \left(\frac{f}{200\ \cancel{MeV}}\right)\left(\frac{\cancel{element}}{1{,}075\ \cancel{g\ U^{235}}}\right)\left(\frac{1.6\ \cancel{g\ U^{235}}}{cm^3}\right)\left(\frac{1}{40\ \cancel{element}}\right) = 1.5 \cdot 10^{21}\ f\ cm^{-3}.$$

This result is identical to the value given at the beginning of this subsection and shows how this fission density was calculated.

The percentage of atoms that underwent fission per initial heavy metal (U) atom is given by

$$\begin{gathered}\left(\frac{1.5 \cdot 10^{21}\ \cancel{f}}{\cancel{cm^3}}\right)\left(\frac{\cancel{cm^3}}{1.6\ \cancel{g\ U^{235}}}\right) \\ \times \left[\left(\frac{\cancel{mol}}{235\ \cancel{g\ U^{235}}}\right) + \left(\frac{100\ \cancel{wt.\%} - 93\ \cancel{wt.\%}}{100\ \cancel{wt.\%}}\right)\left(\frac{\cancel{g\ U^{238}}}{\cancel{g\ U^{235}}}\right)\left(\frac{\cancel{mol}}{238\ \cancel{g\ U^{238}}}\right)\right]^{-1} \\ \times \left(\frac{1\ \cancel{mol}}{6.022 \cdot 10^{23}\ \cancel{atom}}\right)\left(\frac{100\ at.\%\ \cancel{atom}}{\cancel{f}}\right) = 34.2\ at.\%.\end{gathered} \tag{2}$$

This result falls within the range quoted above. However, it is unclear how the volume occupied by the cladding is treated and whether the fissile densities used in the calculations already account for fabrication porosity. Handling these parameters differently could make it difficult to compare calculations to values in the literature.

A third example burnup calculation is included below:

$$\begin{gathered}(250\ \cancel{MW})(60\ \cancel{d})\left(\frac{\cancel{element}}{1{,}075\ \cancel{g\ U^{235}}}\right)\left(\frac{93\ \cancel{wt.\%\ g\ U^{235}}}{100\ \cancel{wt.\%\ g}\ U}\right)\left(\frac{1}{40\ \cancel{element}}\right) \\ \times \left(\frac{10^3\ GW}{\cancel{MW}}\right)\left(\frac{\cancel{g}}{10^3\ \cancel{kg}}\right)\left(\frac{10^3\ \cancel{kg}}{\cancel{MT}}\right) = 324\ GWd/MTU.\end{gathered} \tag{3}$$

Again, this result is of the same magnitude but differs significantly from the value quoted above. More information is needed about the methods used to calculate burnup in the literature, and those methods need to be adopted to maintain consistency.

3.5 IRRADIATION EFFECTS

Fuels similar to that used in ATR have been observed to swell at about $\Delta V/V_0 = 3 \times 10^{-23}\ cm^3 f^{-1} \cdot F$, where ΔV is the change in fuel volume, V_0 is the original fuel volume, and F is the fission density [18]. The rate of swelling has been observed to increase at higher burnups (> 1.5×10^{21} f·cm^{-3}) in some reactors and/or fuels. Swelling appears to be accommodated by fabrication porosity in the fuel via a process called *densification* [23]. Higher swelling rates are observed when reactor temperatures are not high enough to enable densification [18]. Fuel plate growth generally manifests as increases in thickness rather than length [23].

Irradiation experiments have been conducted to assess the ability of uranium aluminide pellets to retain radioactivity [18]. No radioactivity releases were observed when UAl_3 and UAl_4 pellets were irradiated to burnups up to 35 at% at temperatures up to 1,280°C and 730°C, respectively. Similar results were obtained for uranium aluminide pellets irradiated to burnups up to 60 at%. The solidus temperature of Al-6061 cladding is 582°C, so it might be assumed that uranium aluminide dispersant fuel plates can release fission gas above this temperature. For the purposes of this project, tests conducted at this stage of the project should be conducted under the conservative assumption that ATR SNF retains all the fission products produced during operation (accounting for depletion and decay).

ATR fuel assemblies have also been observed to corrode because of reactions with the reactor coolant. Corrosion typically forms aluminum oxides [22].

3.6 FISSION PRODUCT CONTENT

Several studies have been conducted to assess the fission product content of ATR SNF and similar uranium aluminide dispersion fuels. A study which examined fuels like that used in ATR detected significant concentrations of ^{95}Zr, ^{103}Ru, ^{134}Cs, ^{137}Cs, and ^{144}Ce [21]. A second study focused on ATR specifically notes that the fission products of concern in an accident scenario at ATR included gaseous and/or highly volatile Xe, Kr, Cs, I, and Te [27]. The study references fission product inventories calculated using the ORIGEN2 isotope generation and depletion code [28]. Several more recent studies reference the same ORIGEN2 calculations [16, 29].

Papers documenting results of ORIGEN 2 calculations have been published recently, drawing on these calculations to design conversion to LEU fuel [30, 31] . These studies were conducted to estimate the fission product inventory and corresponding activities of an entire ATR core's worth of fuel after 60 days of operation at 250 MW [30]. The calculations were conducted using a cross-section library optimized for the ATR neutron spectrum. Inventories were calculated at times ranging from two hours to one year after shutdown, but the maximum time given in the report is 150 days. Activities are reported for elements and individual nuclides [30]. Elements with activities >1×10^3 Ci at 150 days after shutdown included Pu, Kr, Sr, Y, Zr, Nb, Ru, Rh, Sn, Sb, Te, Cs, Ba, La, Ce, Pr, Pm, and Eu. The full results are available on microfilm.

Byron Curnett reported on power histories of ATF-1 in the ATR. [32]. The work builds on the calculations above by estimating the maximum fission product content a single fuel element. It considers one ATR fuel element operating at 6.25 MW, which is equivalent to 40 fuel elements operating at a total power of 250 MW, for two 60-day cycles. The masses and activities of 808 radionuclides were calculated at times ranging from two hours to 150 days after shutdown. Curnutt noted that realistic ATR operation differs significantly from the idealized case considered therein. ATF fuel elements typically operate at 2.5–3.0 MW for 2–3 ATR cycles before being discharged.

It is recommended that fission product content of each individual fuel element used in ZIRCEX testing be calculated during the early stages of the work. Bounding calculations may be sufficient to ensure adequate fission product control after the process is refined further. These calculations must consider the irradiation history (associated with fission product production) and cooling time (associated with fission product decay) of each fuel element.

These calculations would require the ATR neutron flux. Depending on the accuracy and resolution needed, the neutron flux may need to be resolved spectrally and/or spatially. The calculations could be performed using a combination the MOLE, GRIFFIN, and ORIGEN2 codes. Zain Karriem of the Radioisotope Science and Technology Division, who previously worked on the proposed ATR LEU-conversion project [16], is familiar with the calculations referenced above and this type of work in general. Kyoung Lee of the Nuclear Energy and Fuel Cycle Division also has the expertise and availability needed to perform the calculations.

Per Karriem's recommendation, the authors attempted to locate ATR neutron flux data from the 1994 ATR CIC Benchmark. Some of the benchmark details are covered by Kim and Schnitzler [8], but the benchmark models and data appear to be available only from the International Criticality Safety

Benchmark Evaluation Project (ICSBEP) Handbook [33]. As of 2020, the ICSBEP Handbook contained 582 benchmark specifications for 5,053 reactor configurations [34, 35].

Unfortunately, the ICSBEP Handbook and the ATR model within it were subject to the following restrictions as of 2002 [8]:

> . . . *(1) modeling information and the detailed Monte Carlo N-Particle model will only be used for calculating and studying the results for validation of neutronics computer codes and improvement of basic nuclear cross section data, (2) the model will not be used for any studies other than those mentioned above, and (3) users of the handbook will not distribute the model to anyone outside of their own organization.*

Current restrictions appear to focus on the latter, along with a prohibition about permitting internet access to the ICSBEP Handbook and database [36].

ICSBEP Handbook data were still in use at INL as of 2014 [37], and a subset of the data was used by the Reactor and Nuclear Systems Division (now the Nuclear Energy and Fuel Cycle Division) at ORNL to validate the SCALE code system in 2020 [38]. This suggests that the handbook data could be obtained expeditiously from ORNL sources, if not directly from the Nuclear Energy Agency (NEA).

More general ATR neutron spectrum characterizations based on dosimeter irradiations and neutronics calculations are available in the literature [26]. The study also yielded spectrum-averaged cross sections. These may be helpful for performing and assessing the accuracy of depletion calculations.

Because it will take time to perform fission product inventory calculations, the authors recommend a three-step approach to deliver actionable and continually improving results for use in the ongoing ZIRCEX testing: (1) apply engineering judgement and hand calculations to estimate fission product contents for immediate use, (2) perform averaged fission product content calculations to improve intermediate-term accuracy, and (3) perform calculations using spectrally and/or spatially discretized neutron flux data for long-term use.

The authors recommend the following approaches for defining the needed ATR neutron flux, which are given in order of most preferable to least preferable:

1. Obtain the most recent ICSBEP Handbook from within ORNL or from INL.
2. Obtain additional ATR data from INL and supplement them with data from the open literature, approximations, and assumptions.
3. Survey the open literature for neutron flux data from a comparable reactor and use them to define a surrogate for the current work.

4. OPEN QUESTIONS

Data gaps and open questions are listed below.

1. What is the structure and composition of uranium aluminide fuel before and after burnup?
2. How does U–Al coordination number and structure of the fuel chlorination inform the ZIRCEX process?

3. How might the geometry of a large fuel element, a medium-sized fuel plate, or smaller segmented samples affect chemical processing?

4. What impurities and alloying elements might be concerning during chlorination? At what concentrations do they become a concern?

5. Can the fission product contents of fuels with various cooling times be calculated, and what is their chemical state?

6. What fission products are of concern? Are there specific concerns with volatility, reactivity with Cl, radioactivity, and/or toxicity?

7. What are the ranges of composition, enrichment, burnup, and fission product content that may be encountered during ZIRCEX processing resulting from differences in sample size/geometry, irradiation history, and cooling time?

5. CONCLUSIONS

ATR fuel has been identified as a resource for HALEU production. A survey of published literature describing ATR fuel was performed. However, this fuel type is highly variable, and some of the information on fuel composition and fabrication is proprietary. Therefore, fundamental studies of fuel reprocessing must use a model fuel that represents the main chemical and structural features. For that reason, an UAl_x alloy will be fabricated to use to test the chemical processing. The potential chlorination of UAl_x will be assessed in the advanced chlorination process of Al-8001 and Al-6061. Initial studies will track the alloying elements of the Al, which are Si, Fe, Cu, Mn, Mg, Cr, Zn, and Ti, in addition to the U itself. Further studies will include fission product simulants. Because advanced chlorination solvents include sulfur, the chemistry of sulfur with major and minor constituents will also be investigated. Removal of chlorine from the product is important for downstream processing. This work will allow for the assessment of the feasibility of advanced chlorination to separate aluminum from uranium, including chemical decladding. The fate of the uranium-aluminum alloy under advanced chlorination conditions will also be assessed.

REFERENCES

[1] M. Tschiltz. 2018. “Addressing the challenges with establishing the infrastructure for the front-end of the fuel cycle for advanced reactors”, Nuclear Energy Institute white paper, January 2018. https://www.nei.org/CorporateSite/media/filefolder/resources/reports-andbriefs/white-paper-advanced-fuel-cycle-infrastructure-201801.pdf.

[2] S. Gallier. 2019 (September). “Looking High and Low for HALEU,” *Nuclear News*, 26–29.

[3] T. Todd and J. Campbell. “Hybrid Zirconium Extraction (ZIRCEX) Process - 19-50467-05_R3,” Idaho Falls, Idaho.

[4] S.L. Downie. 2021. “Hybrid Zircex Hydrochlorinator" INL/EXP-21-63685-Revision-0. 1–4.

[5] B. Vestal, J. R. Travis, A. A. Albert, S. H. Bruffey, J. McFarlane, E. D. Colins, R. D. Hunt, and C. E. Barnes. 2023. A novel Protocol to Recycle Zirconium from Zirconium Alloy Cladding from Spent Nuclear Fuel Rods, *J. Nucl. Mater.* 578, https://doi.org/10.1016/j.jnucmat.2023.154339

[6] L. Lacroix, et al. 2017. “Aluminum-Clad Spent Nuclear Fuel: Technical Considerations and Challenges for Extended (>50 years) Dry Storage" - RPT-1575,” Idaho Falls, Idaho.

[7] M. J. Connolly et al. 2017. “ATR Spent Fuel Management Options Study - INL/EXT-16-40471,” Idaho Falls, Idaho.

[8] S. Kim and B. Schnitzler. 2005. “Advanced Test Reactor: Serpentine Arrangement of Highly Enriched Water-Moderated Uranium-Aluminide Fuel Plates Reflected by Beryllium” NEA/NSC/DOC/(95)03/II HEU-MET-THERM-022, Idaho Falls, Idaho.

[9] C. Stanley and F. Marshall. 2008. “Advanced test reactor - a national science user facility INL/CON-07-13310,” in *Proceedings of the 16th International Conference on Nuclear Engineering ICONE16*. 1–6.

[10] F. Marshall. 2005. “Advanced Test Reactor Capabilities and Future Operating Plans - INL/CON-05-00549,” in *Test Research and Training Reactors Annual Meeting.* 1–9.

[11] G. W. Gibson and D. R. deBoisblanc. 1966. “The Use of Uranium Aluminide Powders in Nuclear Reactor Fuel Elements,” *Mod. Dev. Powder Metall.*, 26–35, doi: 10.1007/978-1-4684-7712-2_2.

[12] D.W. Nigg, K.A. Steuhm. 2014. "Advanced Test Reactor core modeling update project, Annual Report for Fiscal Year 2014". Idaho National Laboratory, INL/EXT-14-33319.

[13] M. Graber, G. Gibson, V. Walker, and W. Francis. 1964. *Results of ATR Sample Fuel Plate Irradiation Experiment*. IDO-16958. Idaho Falls, Idaho.

[14] V. Walker, M. Graber, and G. Gibson. 1966. “ATR Fuel Materials Development Irradiation Results -- Part II - IDO-17157,” Idaho Falls, Idaho.

[15] “ATR Extended Burnup Program" ANCR-1015. Idaho Falls, Idaho, 1971.

[16] M. D. DeHart, Z. Karriem, M. A. Pope, and M. P. Johnson. 2018. “Fuel Element Design and Analysis for Potential LEU Conversion of the Advanced Test Reactor,” *Prog. Nucl. Energy*, 104, pp. 117–135. doi: 10.1016/j.pnucene.2017.09.007.

[17] M. A. Pope, M. D. Dehart, S. R. Morrell, R. K. Jamison, E. C. Nef, and D. W. Nigg. 2014. “Enhanced Low-Enriched Uranium Fuel Element for the Advanced Test Reactor - INL/CON-14-33161,” in *RERTR 2014 35th International Meeting on Reduced Enrichment for Research and Test Reactors*. 1–13.

[18] D. Stahl. 1982 (July). “Fuels for Research and Test Reactors, Status Review” ANL-83-5,” Argonne, Illinois.

[19] Gordon, P., and Kaufmann, A. R. 1950 (January). “Uranium-Aluminum and Uranium-Iron,” *J. Met.* 188: 182–194.

[20] A. Dwight. 1982. “A Study of the Uranium-Aluminum-Silicon System - ANL-82-14,” Argonne, Illinois.

[21] L. Miller and J. Beeston. 1986. “Extended Life Alumunide Fuel Final Report - EGG-2441,” Idaho Falls, Idaho.

[22] J. H. Erwin, W. J. Werner, M. M. Martin, 1968. Development and Fabrication of Instrumented-Plate Advanced Test Reactor Fuel Elements, Oak Ridge National Laboratory, ORNL-4268. “Advanced Test Reactor - INEL-MISC-005,” Idaho Falls, Idaho.

[23] M. Graber, G. Hayner, R. Hobbins, and G. Gibson. 1971. “Performance Evaluation of Core II and III Advanced Test Reactor Fuel Elements - ANCR-1027.”

[24] J. McFarlane, D. Benker, D. W. DePaoli, L. K. Felker, and C. H. Mattus. 2015. "Dissolution and Separation of Aluminum and Aluminosilicates," *Separation Science and Technology* 50 (18), 2803–2818.

[25] M. A. Reichenberger, B. J. Walker, L. D. Smith, C. J. Weigel, and J. C. Lowden. 2020. Comparison of Fluence-Rate Determination Technique for the Advanced Test Reactor – Critical Facility, INL/CON-19-53729-Rev 1, International Conference on Advancements in Nuclear Instrumentation Measurement Methods and Their Applications, June 17–21, 2019, Paper 41275.

[26] J. W. Rogers and R. A. Anderl. 1995. ATR Neutron Spectral Characterization, INEL-95/0494.

[27] J. Adams and M. Carboneau. 1991. “Fission Product Transport and Behavior during Two Postulated Loss of Flow Transients in the ATR - EGG-M-91258.”

[28] A. G. Croff. 1983. “ORIGEN2: A Versatile Computer Code for Calculating the Nuclide Compositions and Characteristics of Nuclear Materials,” *Nucl. Technol.*, 62 (3): 335–352. doi: 10.13182/nt83-1.

[29] J. Navarro, R. Aryaeinejad, and D. Nigg. 2011. “A Feasibility Study to Determine Cooling Time and Burnup of ATR Fuel Using a Nondestructive Technique and Three Types of Gamma-Ray Detectors," INL/CON-11-22168.

[30] J.P. Adams, M.L. Carboneau, and D.L. Hagrman. 1993. “Fission product transport and behavior during two postulated loss-of-flow transients in the Advanced Test Reactor", Nuclear Technology 103, 66-78.

[31] M. DeHart, M.A. Pope, D.W. Nigg, R.K. Jamison, S.R. Morrell. 2018. “Fuel element design and analysis for potenital LEU conversion of the Advanced Test Reactor". Progress in Nuclear Energy 104, 117-135.

[32] B.J. Curnutt. 2017. "ATR-1 power histories", Idaho National Laboratory, INL/EXT-17-43909.

[33] J. B. Briggs, L. Scott, and A. Nouri. 2003. “The International Criticality Safety Benchmark Evaluation Project,” *Nucl. Sci. Eng.*, 145 (1): 1–10. doi: 10.13182/NSE03-14.

[34] J. B. Briggs. 2002. “The Activities of the International Criticality Safety Benchmark Evaluation Project (ICSBEP),” *J. Nucl. Sci. Technol.*, 39: 1427–1432. doi: 10.1080/00223131.2002.10875373.

[35] A. Nouri, P. Nagel, J. B. Briggs, and T. Ivanova. 2003. “DICE: Database for the International Criticality Safety Benchmark Evaluation Program handbook,” *Nucl. Sci. Eng.*, 145 (1): 11–19. doi: 10.13182/NSE03-15.

[36] NEA (2020), "ICSBEP Handbook 2020", *International Criticality Safety Benchmark Evaluation Project Handbook* (database), https://doi.org/10.1787/7e0ebc50-en (accessed on 01 March 2023).

[37] G. Palmiotti, J. B. Briggs, T. Kugo, E. Trumble, A. C. Kahler, and D. Lancaster. 2014. "Applications of Integral Benchmark Data," *Nucl. Sci. Eng.*, 178 (3): 295–310. doi: 10.13182/NSE14-33.

[38] T. M. Greene and W. J. Marshall, "SCALE 6.2.4 Validation: Nuclear Criticality Safety," ORNL/TM-2020/1500v2," Oak Ridge, Tennessee, 2020.